

## Electrical properties of $p$ - $n$ junctions based on superlattices of AlN/AlGa(In)N

V. Kuryatkov, K. Zhu, B. Borisov, A. Chandolu, Yu. Gherasoiu, and G. Kipshidze  
*Department of Electrical and Computer Engineering, Texas Tech University, Lubbock, Texas 79409*

S. N. G. Chu  
*Agere Systems, Murray Hill, New Jersey 07974*

M. Holtz  
*Department of Physics and Nano Tech Center, Texas Tech University, Lubbock, Texas 79409*

Yu. Kudryavtsev and R. Asomoza  
*SIMS Laboratory of SEES, Department of Electrical Engineering, CINVESTAV, Mexico Distrito Federal 07300, Mexico*

S. Nikishin<sup>a)</sup> and H. Temkin  
*Department of Electrical and Computer Engineering and Nano Tech Center, Texas Tech University, Lubbock, Texas 79409*

(Received 13 June 2002; accepted 23 June 2003)

Measurements of acceptor activation energy in  $p$ - $n$  junctions based on superlattices of AlN (1.25 nm thick) and Al<sub>0.08</sub>Ga<sub>0.92</sub>(In)N (0.5 nm thick), with the average AlN content greater than 0.6, are reported. Structural characteristics of superlattices were determined using transmission electron microscopy and x-ray diffraction.  $p$ - $n$  junctions in mesa-etched diodes exhibit low leakage current densities of  $3 \times 10^{-10}$  A/cm<sup>2</sup> at near zero bias. Acceptor activation energy of  $207 \pm 10$  meV, obtained from the temperature dependence of the forward current, is very similar to that of uniform alloy of Al<sub>0.08</sub>Ga<sub>0.92</sub>N that constitutes the well material. The acceptor activation energy thus appears controlled by the well material and remains low despite high average AlN content and large band gap. © 2003 American Institute of Physics. [DOI: 10.1063/1.1603333]

Ultraviolet light emitting diodes (LEDs) with emission wavelengths between 340 and 280 nm would open a number of applications, from fluorescence excitation to data storage. Despite recent progress,<sup>1-7</sup> preparation of light sources operating below 300 nm is still very difficult. Limits on  $p$ -type doping of AlGaIn with high Al concentration can be overcome to some extent by the use of superlattices (SLs) of AlGaIn/GaN<sup>8-11</sup> and AlGaInN/AlGaInN.<sup>4</sup> Recently, we have shown that SLs based on AlN/AlGaInN, doped with Mg, can be used as a large band gap  $p$ -type cladding layer, demonstrating a 280 nm LED.<sup>7,8</sup>

In this letter we discuss electrical properties of  $p$ - $n$  junctions based on AlN/AlGaInN SLs. The SL-based structures were grown on sapphire using gas source molecular beam epitaxy<sup>12</sup> with ammonia. The samples were analyzed with secondary ion mass spectrometry (SIMS), transmission electron microscopy (TEM), atomic force microscopy (AFM), and x-ray diffraction. Room temperature Hall measurements showed hole concentrations in  $p$ -type AlN/AlGaInN SLs of  $1 \times 10^{18}$  cm<sup>-3</sup>, with the resistivity of  $\sim 5$ -6  $\Omega$  cm, and electron concentrations in  $n$ -type AlN/AlGaInN SLs of  $3 \times 10^{19}$  cm<sup>-3</sup>, with the resistivity of  $0.015 \pm 0.005$   $\Omega$  cm.<sup>7,8</sup> These concentrations and resistivities reflect primarily the in-plane transport in SLs and detailed electrical measurements on mesa-etched diodes are needed, as discussed later, to determine the out of plane component.

The growth started with a layer of AlN, 40 nm-thick, followed by a 1- $\mu$ m-thick buffer layer of GaN. This GaN layer was incorporated in order to reduce dislocation density in the device SL. Dislocation density in the top part of the GaN layer was estimated from TEM measurements at  $\sim 6 \times 10^9$  cm<sup>-2</sup>. The SL-based device structure with a thickness of  $\sim 0.7$   $\mu$ m (for a total of 330 periods) was grown over the GaN layer. The AlN barriers were 1.25 nm thick and the AlGaInN wells were 0.5 nm thick in both  $p$ - and  $n$ -type SLs. In LED structures, an active region consisting of five undoped barrier/well pairs with the well thickness increased to 0.75 nm, was placed between the  $n$ - and  $p$ -type SLs. It should be remembered that the average thickness of a monolayer (ML) of AlN and GaN is 0.25 nm. Barriers are thus 5 ML thick and wells are 2 and 3 ML thick. These thicknesses are below the critical layer thickness.<sup>13</sup> No additional dislocations were indeed observed in the SL structure by TEM.<sup>7</sup>

A TEM cross section of the active region of the LED structure is shown in Fig. 1(a). All the layers appear flat and well defined, with abrupt interfaces. The average thickness determined from TEM data is in good agreement with estimates based on growth calibrations. Figure 1(b) shows a higher magnification image of the active region. The five undoped wells are indeed wider, as intended. The overall flatness of the SL structure is confirmed by AFM measurements. In a  $10 \times 10$   $\mu$ m scan the rms roughness of  $\sim 0.5$  nm was obtained. This is similar to the roughness measured on uniform layers of Al<sub>0.08</sub>Ga<sub>0.92</sub>N of similar thickness.

The average AlN content of our SLs was determined by

<sup>a)</sup>Author to whom correspondences should be addressed; electronic mail: sergev.nikishin@coe.ttu.edu

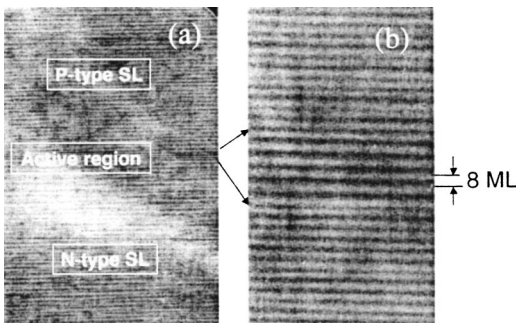


FIG. 1. TEM cross section of: (a) a central portion of a superlattice structure of an ultraviolet LED and (b) an active region at higher magnification.

x-ray diffraction. Figure 2 shows a (0002) rocking curve obtained on the entire device structure. The strong GaN reflection is due to the 1- $\mu\text{m}$ -thick buffer layer. The thin nucleation layer of AlN contributes a much broader and weaker peak. The AlN/AlGaInN superlattice produces a well-defined reflection consistent with an average AlN content of  $\sim 0.63$ . The reflection is somewhat broadened, suggesting that about 15% of the barriers may be, on the average, a monolayer thicker than the design goal of 5 ML. The overall AlN content measured by x-ray diffraction is consistent with the well and barrier thicknesses measured by TEM cross sections. The weaker structure near  $\theta \sim 16.58^\circ$  is likely associated with GaInN and its presence may indicate some degree of phase separation in the wells, despite low average concentration of indium.

The lower SL structure is doped with Si derived from silane. This *n*-type doping process is very effective and the dopant is introduced only intermittently, during the growth of AlGaInN wells. The average Si concentration, measured by SIMS, was  $\sim 10^{20} \text{ cm}^{-3}$ . This is in good agreement with Hall measurements of the electron concentration ( $n \sim 3 \times 10^{19} \text{ cm}^{-3}$ ), indicating excellent activation efficiency of Si. This result is also consistent with recent report of highly doped *n*-type AlN/GaN SLs.<sup>14</sup> SIMS measurements of *p*-type SLs showed the average Mg concentration in AlGaInN wells of  $\sim 10^{20} \text{ cm}^{-3}$ , assuming no Mg incorporation in AlN barriers. This is consistent with Hall measurements of the hole concentration ( $n \sim 1 \times 10^{18} \text{ cm}^{-3}$ ), showing Mg activation efficiency of about 1%, similar to that measured in uniform alloy of  $\text{Al}_{0.08}\text{Ga}_{0.92}\text{N}$ .<sup>15-17</sup> The same alloy is used for wells in our SL structure. Because of the high growth temperature, the InN content in our wells is

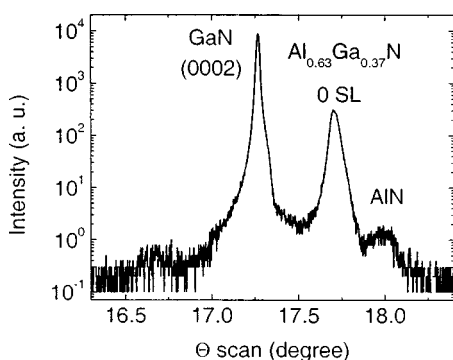


FIG. 2. X-ray diffraction rocking curve obtained on a superlattice LED structure.

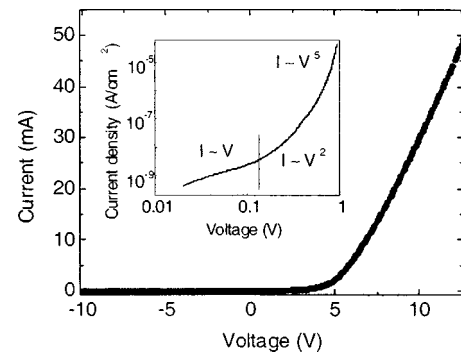


FIG. 3. Room-temperature current-voltage characteristics of a mesa-defined *p-n* junction. The inset details the low-forward-bias range (log-log). Below 0.12 V we see that  $I-V$  (linear regime).

quite low. SIMS measurements show approximately  $10^{17} \text{ cm}^{-3}$  In atoms in the SL structure. The amount added is small enough not to reduce the band gap or to alter the period of the superlattice but it results in improved luminescence efficiency.<sup>8</sup> It has been argued recently that even small amounts of In in the lattice may have important effect on the interfacial electric field<sup>18</sup> and therefore electrical properties of the SL.

In order to distinguish between the in-plane and out-of-plane conduction electrical measurements were carried out on mesa-defined diodes. The mesas, 110  $\mu\text{m}$  in diameter, were plasma etched with  $\text{Cl}_2$  chemistry using Ni contacts as masks.<sup>16</sup> Ohmic contacts to *p*- and *n*-type SLs were prepared with Ni/Au and Ti/Al/Ti/Au, respectively. High doping levels allowed us to fabricate Ohmic contacts to *p*-type and *n*-type material without high temperature anneals. The  $I-V$  characteristics representative of our superlattice diodes are plotted in Fig. 3. The device turns on at  $\sim 5.0$  V, consistent with the active layer band gap of  $\sim 4.8$  eV. Very low dark leakage currents, 2–3 pA ( $\sim 3 \times 10^{-10} \text{ A/cm}^2$ ), were measured near zero bias, indicative of high quality junction and low etch-induced damage on the mesa sidewalls. The reverse leakage current remained below 200  $\mu\text{A}$  up to a bias of  $-10$  V. The leakage current scales with the area of the diode, not its perimeter, and the surface leakage component thus appears negligible. The diodes have breakdown voltages in excess of  $-90$  V. The presence of the active layer does not alter their electrical characteristics.

Above the turn-on voltage current increases linearly with bias to at least 100 mA, reaching peak current density greater than  $1 \text{ kA/cm}^2$ . The differential series resistance scales with the mesa area, from  $\sim 45\text{--}50 \Omega$  in 350  $\mu\text{m}$  devices to  $\sim 110\text{--}130 \Omega$  in 110  $\mu\text{m}$  diodes. The resistance  $R_m$  of mesa diodes can be written as a sum of the contact ( $R_c$ ), spreading ( $R_s$ ), and vertical ( $R_v$ ) resistances. The resistance of the etched part of the mesa, corresponding to transport across the SL layers is  $R_v \sim \rho_\perp h/A$ , where  $\rho_\perp$  is the perpendicular resistivity of the SL,  $h$  is the height on the mesa ( $\sim 0.5 \mu\text{m}$ , with the thickness of *p*-SL  $\sim 0.4 \mu\text{m}$ ), and  $A$  its area. The contact resistance of a 110  $\mu\text{m}$  diode, calculated from an independent measurement of specific contact resistance, is  $R_c \sim 90 \Omega$ . Assuming higher lateral conductivity in the *n*-type SL (obtained from Hall measurements) and neglecting  $R_s$ , we obtain  $R_v \sim 20 \Omega$  resulting in  $\rho_\perp \sim 40 \Omega \text{ cm}$  for *p*-SL. Comparing this to the in-plane conductivity ( $\rho$ ) of *p*-SL obtained

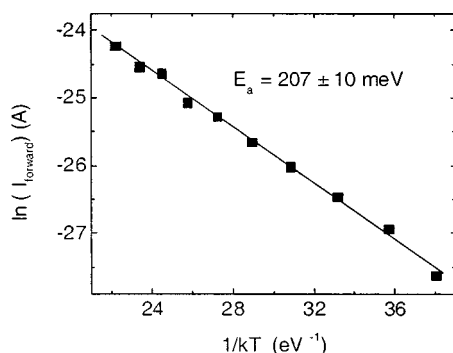


FIG. 4. Temperature dependence of the forward current obtained at a bias of 0.1 V. Acceptor activation energy of  $207 \pm 10$  meV is within experimental error of that measured previously on  $p$ - $n$  junctions of  $\text{Al}_{0.08}\text{Ga}_{0.92}\text{N}$ .

from Hall measurements,  $\rho \sim 5\text{--}6 \Omega \text{ cm}$ , we obtain the conductivity anisotropy  $\rho_{\perp}/\rho \sim 6\text{--}8$ . These simple considerations indicate relatively low  $\rho_{\perp}$ , considering the high AlN fraction in our SLs, and the importance of reducing the  $p$ -contact resistance.

In LED structures light emission is observed above the turn-on voltage. For different diodes fabricated on 2 in. diameter wafers the wavelength of emission varies in the range of 279–282 nm. This spread is attributed to variations in the barrier and well thickness in the active region.

The inset of Fig. 3 shows the details of the current–voltage characteristics at low forward voltages ranging from 0.01 to 1 V. We find a linear dependence of diode current on forward voltage below 0.12 V. We can also conclude that at forward voltages above 0.2 V space-charge recombination dominates the current transport. This is similar to homojunction diodes of GaN<sup>17</sup> and indeed, while our diodes are based on short period superlattices, we consider them to be homojunctions in the sense that both  $n$  and  $p$  sides have the same average band gaps. Unusually, the depletion edge is located in the region with position-dependent electric field and free-hole concentrations and this may result in considerable deviations from homojunction behavior.

The temperature dependence of the forward diode current in AlGaIn is determined by the ionization energy of acceptors. This is because the forward current under low forward bias, in the linear regime, is directly proportional to the density of thermally excited holes.<sup>19,20</sup> This method yields reliable acceptor activation energies in homojunction diodes based on GaN and AlGaIn.<sup>16,17,20</sup> Measurements of the temperature dependence of the forward current in SL-based junctions, at a constant bias of 0.1 V, are illustrated in Fig. 4. Current–voltage characteristics of mesa diodes were measured in the temperature range of 20–250 °C. Linear  $I$ – $V$  relationship was observed below 0.12 V at each temperature studied. The Arrhenius plot of the forward current, shown in Fig. 4, gives the acceptor activation energy of  $207 \pm 10$  meV. This is in excellent agreement with our previous measurements of the acceptor activation energy in random alloy of  $\text{Al}_{0.08}\text{Ga}_{0.92}\text{N}$ .<sup>15,17</sup> This result implies that the holes in our  $p$ -type SL structures are contributed only by the wells and that the conduction through the AlN barriers is by tunneling, i.e., it does not contribute any additional temperature dependence. While the relative contributions of interfacial electric

field and strain in distorting the band structure and assisting in the tunneling are not yet well understood, the AlN/AlGaInN SL structure described here is very effective in producing low effective values of the acceptor activation energy.

Work at Texas Tech University is supported by DARPA (Dr. J. Carrano), NSF (ECS-0070240 and ECS-9871290), US Army SBCCOM, NATO-Science for Peace (SfP 974505), and the J. F. Maddox Foundation.

- <sup>1</sup>K. Tadamoto, H. Okagawa, Y. Ohuchi, T. Tsunekawa, Y. Imada, M. Kato, and T. Taguchi, *Jpn. J. Appl. Phys., Part 2* **40**, L583 (2001).
- <sup>2</sup>T. Nishida, H. Saito, and N. Kobayashi, *Appl. Phys. Lett.* **78**, 3927 (2001); **79**, 711 (2001); N. Kobayashi, T. Nishida, T. Akasaka, S. Ando, and H. Saito, *4th Int. Symp. On Blue Laser and Light Emitting Diodes (ISLLED-2002), 11–15 March 2002, Cordoba, Spain* (2002), p. FrA1.
- <sup>3</sup>A. Kinoshita, H. Hirayama, M. Ainoya, Y. Aoyagi, and A. Hirata, *Appl. Phys. Lett.* **77**, 175 (2000); H. Hirayama, A. Kinoshita, and Y. Aoyagi, *RIKEN Rev.* **33**, 28 (2001); H. Hirayama, A. Kinoshita, A. Hirata, and Y. Aoyagi, *Phys. Status Solidi A* **188**, 83 (2001); H. Hirayama, Y. Enomoto, A. Kinoshita, A. Hirata, and Y. Aoyagi, *Appl. Phys. Lett.* **80**, 37 (2002); H. Hirayama, A. Kinoshita, A. Hirata, and Y. Aoyagi, *4th Int. Symp. On Blue Laser and Light Emitting Diodes (ISLLED-2002), 11–15 March 2002, Cordoba, Spain* (2002), p. FrB2.
- <sup>4</sup>M. A. Khan, V. Adivarahan, J. Zhang, Q. Chen, E. Kuokstis, A. Chitnis, M. Shatalov, J. Yang, and G. Simin, *Jpn. J. Appl. Phys., Part 2* **40**, L1308 (2001); V. Adivarahan, A. Chitnis, J. P. Zhang, M. Shatalov, J. W. Yang, G. Simin, and M. A. Khan, *Appl. Phys. Lett.* **79**, 4240 (2001); A. Chitnis, V. Adivarahan, M. Shatalov, J. Zhang, M. Gaevski, W. Shuai, R. Pachipulusu, J. Sun, K. Simin, G. Simin, J. Yang, and M. A. Khan, *Jpn. J. Appl. Phys., Part 2* **41**, L320 (2002); V. Adivarahan, J. Zhang, A. Chitnis, W. Shuai, J. Sun, R. Pachipulusu, M. Shatalov, and M. A. Khan, *ibid.* **41**, L435 (2002); M. A. Khan, V. Adivarahan, J. P. Zhang, C. Chen, E. Kuokstis, A. Chitnis, M. Shatalov, J. W. Yang, G. Simin, R. Gaska, and M. S. Shur, *4th Int. Symp. On Blue Laser and Light Emitting Diodes (ISLLED-2002), 11–15 March 2002, Cordoba, Spain* (2002), p. LNP3.
- <sup>5</sup>R. D. Dupuis, T. G. Zhu, J. C. Denyszyn, U. Chowdhury, and M. M. Wong, *4th Int. Symp. On Blue Laser and Light Emitting Diodes (ISLLED-2002), 11–15 March 2002, Cordoba, Spain* (2002), p. THC3.
- <sup>6</sup>S. Kamiyama, M. Iwaya, S. Takanami, S. Terao, A. Miyazaki, H. Amano, and I. Akasaki, *Phys. Status Solidi A* **192**, 296 (2002).
- <sup>7</sup>G. Kipshidze, V. Kuryatkov, B. Borisov, S. Nikishin, M. Holtz, S. N. G. Chu, and H. Temkin, *Phys. Status Solidi A* **192**, 286 (2002).
- <sup>8</sup>G. Kipshidze, V. Kuryatkov, B. Borisov, M. Holtz, S. Nikishin, and H. Temkin, *Appl. Phys. Lett.* **80**, 3682 (2002); G. Kipshidze, V. Kuryatkov, K. Zhu, B. Borisov, M. Holtz, S. Nikishin, and H. Temkin, *J. Appl. Phys.* **93**, 1363 (2003).
- <sup>9</sup>E. F. Schubert, W. Grieshaber, and I. D. Goepfert, *Appl. Phys. Lett.* **69**, 3737 (1996).
- <sup>10</sup>P. Kozodoy, M. Hansen, S. P. DenBaars, and U. K. Mishra, *Appl. Phys. Lett.* **74**, 3681 (1999).
- <sup>11</sup>K. Kumakura and N. Kobayashi, *Jpn. J. Appl. Phys., Part 2* **38**, L1012 (1999).
- <sup>12</sup>M. B. Panish and H. Temkin, *Gas Source Molecular Beam Epitaxy* (Springer, Berlin, 1993).
- <sup>13</sup>A. D. Bykhovskii, B. L. Gelmont, and M. S. Shur, *J. Appl. Phys.* **78**, 3691 (1995).
- <sup>14</sup>S. Yamaguchi, Y. Iwamura, Y. Watanabe, M. Kosaki, Y. Yukawa, S. Nitta, S. Kamiyama, H. Amano, and I. Akasaki, *Appl. Phys. Lett.* **80**, 802 (2002).
- <sup>15</sup>S. Nikishin, G. Kipshidze, V. Kuryatkov, K. Choi, İ. Gherasoiu, L. Grave de Peralta, A. Zubrilov, V. Tretyakov, K. Copeland, T. Prokofyeva, M. Holtz, R. Asomoza, Yu. Kudryavtsev, and H. Temkin, *J. Vac. Sci. Technol. B* **19**, 1409 (2001).
- <sup>16</sup>V. V. Kuryatkov, G. D. Kipshidze, S. A. Nikishin, P. W. Deelman, and H. Temkin, *Phys. Status Solidi A* **188**, 317 (2001).
- <sup>17</sup>G. Kipshidze, V. Kuryatkov, B. Borisov, Yu. Kudryavtsev, R. Asomoza, S. Nikishin, and H. Temkin, *Appl. Phys. Lett.* **80**, 2910 (2002).
- <sup>18</sup>I. Lo, J. K. Tsai, L.-W. Tu, K. Y. Hsieh, M. H. Tsai, C. S. Liu, J. H. Huang, S. Elhamri, W. C. Mitchel, and J. K. Sheu, *Appl. Phys. Lett.* **80**, 2684 (2002).
- <sup>19</sup>N. I. Kuznetsov and K. G. Irvine, *Semiconductors* **32**, 335 (1998).
- <sup>20</sup>K. L. Ashley and A. G. Milnes, *J. Appl. Phys.* **35**, 369 (1964).